Cell Calcium 54 (2013) 395–403

Contents lists available at ScienceDirect

Cell Calcium

journal homepage: www.elsevier.com/locate/ceca

FRET-based sensor analysis reveals caveolae are spatially distinct Ca^{2+} stores in endothelial cells☆

Masashi Isshiki[a,*], Mitsuhiro Nishimoto[a,b], Risuke Mizuno[a], Toshiro Fujita[b]

[a] Department of Molecular Vascular Endocrinology, Graduate School of Medicine, The University of Tokyo, Tokyo 113-8655, Japan
[b] Division of Clinical Epigenetics, Research Center for Advanced Science and Technology, The University of Tokyo, Tokyo 113-8655, Japan

ARTICLE INFO

Article history:
Received 15 February 2013
Received in revised form
17 September 2013
Accepted 18 September 2013
Available online 29 September 2013

Keywords:
FRET
Cameleon
Ca^{2+} regulation
Endothelial cells
Vascular endothelial function

ABSTRACT

Ca^{2+}-regulating and Ca^{2+}-dependent molecules enriched in caveolae are typically shaped as plasmalemmal invaginations or vesicles. Caveolae structure and subcellular distribution are critical for Ca^{2+} release from endoplasmic reticulum Ca^{2+} stores and for Ca^{2+} influx from the extracellular space into the cell. However, Ca^{2+} dynamics inside caveolae have never been directly measured and remain uncharacterized. To target the fluorescence resonance energy transfer (FRET)-based Ca^{2+} sensing protein D1, a mutant of cameleon, to the intra-caveolar space, we made a cDNA construct encoding a chimeric protein of lectin-like oxidized low-density lipoprotein receptor 1 (LOX-1) and D1 (LOXD1). Immunofluorescence and immunoelectron microscopy confirmed that a significant portion of LOXD1 was localized with caveolin-1 at morphologically apparent caveolar vesicles in endothelial cells. LOXD1 detected ATP-induced transient Ca^{2+} decreases by confocal FRET imaging in the presence or absence of extracellular Ca^{2+}. This ATP-induced Ca^{2+} decrease was abolished following knockdown of caveoin-1, suggesting an association with caveolae. The X-ray spectra obtained by the spot analysis of electron-opaque pyroantimonate precipitates further confirmed that ATP-induced calcium decreases in intra-caveolar vesicles. In conclusion, subplasmalemmal caveolae function as Ca^{2+}-releasable Ca^{2+} stores in response to ATP. This intracellular local Ca^{2+} delivery system may contribute to the complex spatiotemporal organization of Ca^{2+} signaling.

1. Introduction

Intracellular calcium is a second messenger that mediates a variety of important functions in vascular endothelial cells, ranging from the production of vasoactive substances to gene expression [1]. A key feature of intracellular calcium (Ca^{2+}) signaling is its complex spatiotemporal organization, which is essential for enabling diverse and versatile cellular functions [2,3].

Caveolae are cholesterol-enriched small plasmalemmal invaginations or subplasmalemmal vesicles, and have been suggested to act as signaling scaffolds based on biochemical and morphological presentation of a diverse array of signaling molecules at the microdomains [4]. Using the chelating-type Ca^{2+} indicator dye indo-1, we previously observed that ATP-induced Ca^{2+} waves originate at caveolin-rich cell edges and are propagated throughout the entire cell [5]. We also demonstrated that caveolae are preferential sites for store-operated Ca^{2+} entry by targeting a fluorescence resonance energy transfer (FRET)-based Ca^{2+}-sensing protein to the cytoplasmic face of caveolae [6]. Thus, many observations, including ours, have suggested that the structure and subcellular distribution of caveolae are critical for Ca^{2+} release from endoplasmic reticulum (ER) Ca^{2+} stores and for Ca^{2+} influx from the extracellular space into the cell [7–9]. However, Ca^{2+} dynamics inside caveolae have never been directly observed and remain uncharacterized.

A variety of Ca^{2+}-regulating and Ca^{2+}-dependent molecules such as IP_3 receptor-like protein [10], Ca^{2+}-ATPase [11] and endothelial nitric oxide synthase (eNOS) [12] are enriched in caveolae, which are known to be mobile and are typically shaped as plasmalemmal invaginations or vesicles. About two decades ago, Dr. Fujimoto detected the colocalization of IP_3 receptor-like protein and Ca^{2+}-ATPase in endothelial caveolae by immunoelectron microscopy, and proposed that caveolae could work as subcompartments of

Abbreviations: LOX-1, lectin-like oxidized low-density lipoprotein receptor 1; ER, endoplasmic reticulum; IP_3, inositol 1,4,5-trisphosphate.

* Corresponding author at: Department of Molecular Vascular Endocrinology, Graduate School of Medicine, The University of Tokyo, 7-3-1 Hongo, Bunkyo-ku, Tokyo 113-8655, Japan. Tel.: +81 3 3815 5411x35733; fax: +81 3 5800 9738.
E-mail address: isshiki-tky@umin.ac.jp (M. Isshiki).

0143-4160/$ – see front matter © 2013 The Authors. Published by Elsevier Ltd. All rights reserved.
http://dx.doi.org/10.1016/j.ceca.2013.09.002

Ca^{2+}-releasable Ca^{2+} stores similar to the major Ca^{2+} store compartment in the ER. However, Ca^{2+} dynamics inside caveolae remain uncharacterized in intact cells.

The goal of this study was to directly measure and analyze Ca^{2+} changes, not at the cytoplasmic face of caveolae but inside subplasmalemmal caveolar vesicles, and to examine whether caveolae work as Ca^{2+}-releasable Ca^{2+} store subcompartments.

2. Materials and methods

2.1. Solutions and chemicals

For experiments that required physiological Ca^{2+}, we used Hank's balanced salt solution (HBSS; Invitrogen, Carlsbad, CA, USA) containing 1.2 mol/L Ca^{2+}, 1.05 mmol/L $MgCl_2$, and 0.83 mmol/L $MgSO_4$. For experiments that required Ca^{2+}-free conditions, we used HBSS without Ca^{2+} and Mg^{2+} supplemented with 1.05 mmol/L $MgCl_2$ and 0.83 mmol/L $MgSO_4$. ATP was from Sigma–Aldrich (St. Louis, MO, USA). Ionomycin was from Calbiochem (San Diego, CA, USA). Caveolin pAb was from BD Biosciences (Franklin Lakes, NJ, USA). GFP mAb and Alexa-conjugated secondary antibodies were from Invitrogen. Anti-clathrin heavy chain pAb (P1663) was from Cell Signaling Technology, Inc. (Boston, MA, USA). Anti-TGN46 pAb was from Abcam® (Cambridge, MA, USA). MitoTracker® Red CMXRos was from Invitrogen. Calreticulin pAb (PA3-900) was from Pierce Biotechnology® (Lockford, IL, USA).

2.2. Cell culture

Endothelial cells were isolated from the descending thoracic aorta of a bovine fetus and maintained in M199-based medium (Invitrogen) as previously described [5].

2.3. Vectors and transfection

The vectors for D1ER, an ER-targeting version of cameleon, GCaMP3 [13], and a red genetically encoded calcium indicator for optimal imaging (RGECO) [14] were kindly provided by Drs. R. Tsien (Howard Hughes Medical Institute, UCSD, La Jolla, CA, USA), L. Looger (Howard Hughes Medical Institute, Ashburn, VA, USA), and R.E. Campbell (University of Alberta, Edmonton, Alberta, Canada), respectively. TagRFP was from Evrogen (Moscow, Russia). We fused the cDNA of D1, a yellow cameleon mutant [15], at the C-terminus of bovine low-density lipoprotein receptor 1 (LOX-1), and inserted it into pcDNA3 (Invitrogen) using the Hind III and Eco RI site. We named this construct LOXD1 (Fig. 1A). Human caveolin1-specific shRNA (AGAGCTTCCTGATTGAGATTCAGTGCATC) (cat# TF314183) and the scrambled negative control non-effective shRNA expression cassette (cat# TR30015) in the pRFP-C-RS plasmid were from Orinene Technologies, Inc. (Rockville, MD, USA). A vector for mitGC3, a mitochondria-targeting version of GCaMP3, was made by insertion of a sequence encoding the N-terminal mitochondrial-targeting sequence of cytochrome c oxidase VIII at the 5′ site of GCaMP3 in the pcDNA3 vector. Sub-confluent endothelial cells were transiently transfected with the indicated cDNA-encoding plasmid using lipofectamine 2000 (Invitrogen) according to the manufacturer's instructions. Two days after transfection, the cells were transferred to 35-mm glass-bottom culture dishes (MatTec Corp, Ashland, MA, USA).

2.4. Imaging

All fluorescence images were captured using a Leica confocal microscopy system TCS SP2 or a TCS SP8 (Leica, Mannheim, Germany) equipped with Acousto-Optical Tunable Filter (AOTF), inverted microscope, and oil immersion objectives of 100× and 40× (PL APO, Leica) with NA values of 1.4 and 1.25, respectively [16]. Excitation lasers were argon (458, 476, 488, 496, and 514 nm lines) and HeNe (543 and 633 nm lines) for SP2, and solid lasers (448, 488, 552, and 638 nm lines) for SP8. For cytosolic $[Ca^{2+}]_i$ imaging, cells transfected with RGECO were excited at 543 nm and emissions ranging from 560 to 600 nm were collected and saved. For mitochondrial $[Ca^{2+}]_i$ imaging, cells transfected with mitG-CaMP3 were excited at 488 nm and emissions ranging from 500 to 530 nm were collected and saved. For subcellular Ca^{2+} imaging in caveolae or the ER, cells transfected with LOXD1 or D1ER were excited at 458 nm using the SP2 system or 448 nm using the SP8 system, and image pairs of donor Cyan Fluorescent protein (CFP) (480 ± 10 nm) and acceptor Citrine or Yellow Fluorescent Protein (YFP) (515 ± 10 nm) were acquired simultaneously. We designated the Citrine (YFP)/CFP emission ratio, which is a measure of bound Ca^{2+}, as the FRET image. Alternate Ca^{2+} recordings of bulk cytosol and another subcellular compartment were performed in cells doubly transfected with RGECO and another Ca^{2+} probe at intervals of 2.44 s. Acquired values of the FRET ratio (R), and the fluorescence (F) were divided by an initial ratio (Ro) or fluorescence (Fo) at $t = 0$ s and plotted as time course graphs. Image processing was performed off-line using Openlab v.5.5.1 (Improvision Ltd., Coventry, UK) software for image handling and processing.

2.5. Immunofluorescence microscopy

Cells were washed three times with phosphate-buffered saline (PBS) and fixed for 30 min at room temperature (RT) with 3% (w/v) paraformaldehyde. After fixation, the cells were rinsed with PBS, with or without permeabilization using 0.1% (v/v) Triton X-100 in PBS for 5 min on ice. Cells were washed extensively with PBS in 0.5% bovine serum albumin (BSA) before processing for indirect immunofluorescence localization [5] of caveolin-1, clathrin heavy chain, TGN46, or mutants of GFPs (CFP and citrine) which are components of LOXD1 exposed to the extracellular space. Cells were examined with the Leica confocal microscope.

2.6. Immunoelectron microscopy

Cultured cells were fixed with 4% (w/v) paraformaldehyde in 0.1 M PBS for 2 h on ice and then permeabilized with 0.1% (v/v) Triton X-100 in PBS for 5 min at RT. Following washes with 10 mM glycine in PBS for 10 min at RT and blocking with 4% (w/v) BSA in PBS for 10 min, primary antibodies against caveolin pAb and GFP mAb in blocking buffer were applied at 4 °C for 24 h. Colloidal gold-conjugated secondary antibodies (BB International, Cardiff, UK) were applied for 24 h. Cells were then extensively washed with PBS and fixed with 2.5% (v/v) glutaraldehyde in 0.1 M PBS and then 1% (w/v) osmium tetroxide (OsO_4) at RT for 30 min each. Fixed cells were dehydrated, embedded in resin, and then ultra-thin sectioned. Samples were observed using transmission electron microscopy (H-700; Hitachi Ltd., Tokyo, Japan) at an acceleration voltage of 75 kVm, and the magnification was set at 30,000×.

2.7. X-ray microanalysis by pyroantimonate methods

Samples were fixed with 1% (w/v) OsO_4 containing 2% (w/v) pyroantimonate potassium ($K[Sb(OH_6)]$) in 0.1 M cacodylate buffer at 4 °C for 60 min. The samples were dehydrated through a series of graded concentrations of ethanol. The samples were transferred to resin (Quetol-812; Nisshin EM Co., Tokyo, Japan) and polymerized at 60 °C for 48 h. The blocks were ultra-thin sectioned at 100 nm

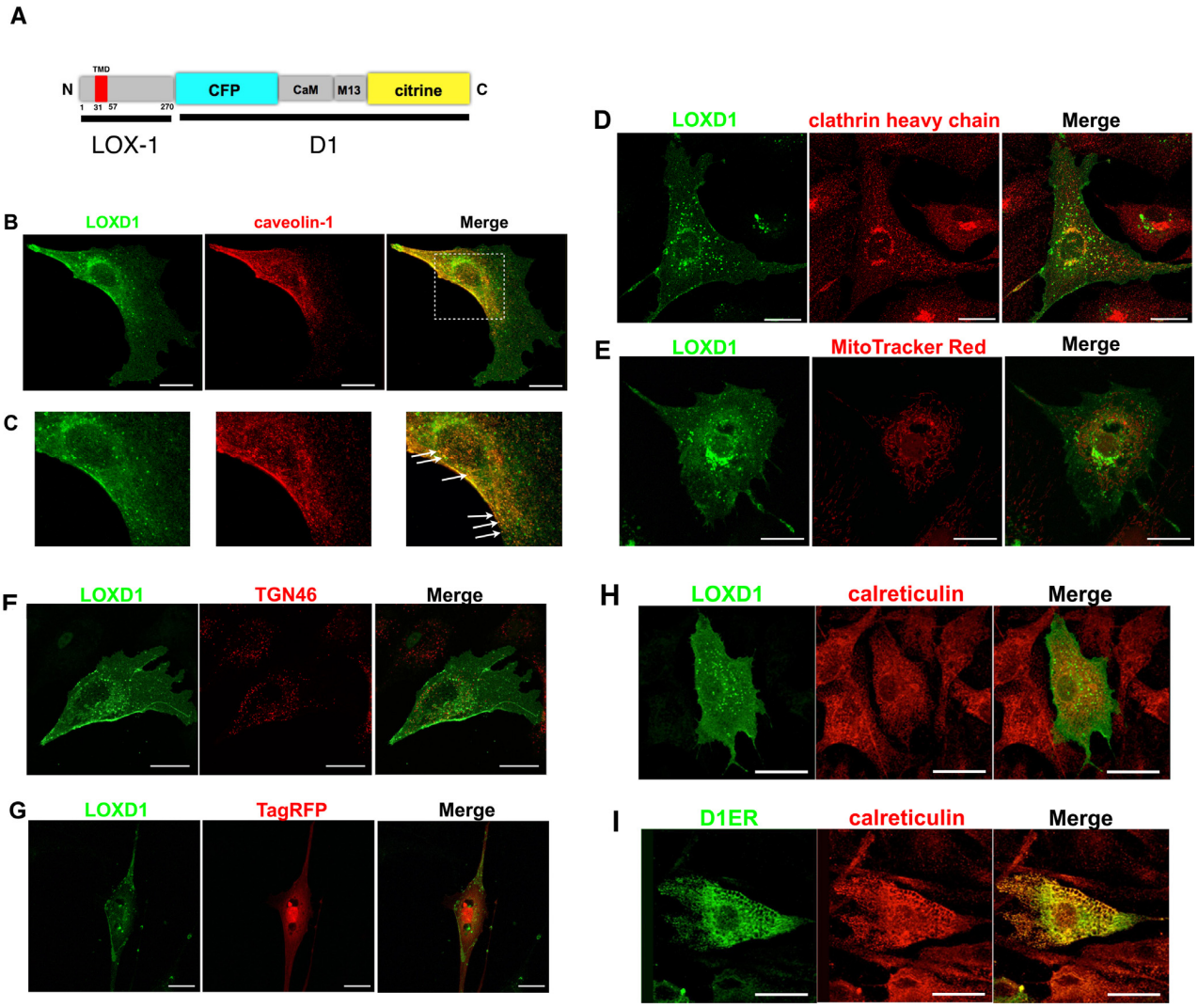

Fig. 1. Construct and subcellular localization of LOXD1. (A) A construct map for LOXD1, consisting of lectin-like oxidized LDL receptor-1 (LOX-1) and D1, a mutant of the genetically encoded FRET-based Ca^{2+} sensing protein. TMD, trans-membrane domain of LOX-1; CaM, calmodulin; M13, calmodulin-binding peptide. (B) A cultured bovine endothelial cell expressing LOXD1 (green) was immunostained for endogenous caveolin-1 (red). Intrinsic CFP fluorescence of LOXD1 was recorded (excitation at 448 nm, emission from 455 to 490 nm) and assigned as a green channel (LOXD1, left panel). Caveolin immunofluorescence was detected by an AlexaFluor 555®-conjugated secondary antibody (excitation at 552 nm, emission from 565 to 600 nm) and assigned as the red channel (caveolin-1, middle panel). (C) An image field surrounded by a dotted rectangle in B was magnified. The merged image indicates that a significant portion of LOXD1 was colocalized with caveolin-1 (arrows). Other control subcellular structures and markers including a clathrin heavy chain (D), mitochondria (E), trans-Golgi network (E), cytosol (G), and endoplasmic reticulum (H) were distinctively localized from LOXD1. (I) Immunofluorescence for calreticulin, a marker of the ER, clearly colocalized with D1ER, an ER-targeted version of the Ca^{2+}-sensing protein. Bar = 10 μm.

with a diamond knife using the LKB Bromma 2088 Ultrotome V (Leica Instruments, Bannockburn, IL) and sections were placed on copper grids. Sections were stained with 2% (w/v) uranyl acetate at RT for 15 min, and then rinsed with distilled water followed by incubation in lead stain solution (Sigma–Aldrich) at RT for 3 min. The grids were observed by transmission electron microscopy (JEM-1200EX; JEOL Ltd., Tokyo, Japan) at an acceleration voltage of 80 kV. Digital images (2048 × 2048 pixels) were taken with a CCD camera (Veleta; Olympus Soft Imaging Solutions GmbH). To confirm that regions of interest contained high amounts of calcium, X-ray microanalysis of calcium precipitation was performed using a transmission electron microscope (JEM-2010; JEOL Ltd.) equipped with energy dispersive X-ray spectrometry. For microanalysis, magnification was set at 15,000× and the area for analysis was exposed to an electron beam for 90 s. The obtained X-ray spectrum was analyzed.

3. Results

Immunofluorescence confocal microscopy confirmed that a significant portion of LOXD1 was colocalized with endogenous caveolin-1, a marker protein of caveolae, in cultured bovine aortic endothelial cells transiently expressing LOXD1 (Fig. 1B and C). The portion of Ca^{2+} sensor D1 was fused to the C-terminal extracellular domain of LOX-1 (Fig. 1A), and some D1 was actually expressed outside of the plasma membrane (Supplemental Figs. S1 and S2). Therefore, the FRET status of the LOXD1 exposed to the extracellular space should remain unchanged if we did not modify Ca^{2+} levels in the extracellular medium. Thus, Ca^{2+} signal changes were detected by LOXD1 in endocytosed vesicles not directly exposed to extracellular medium (Supplemental Fig. S2). In contrast to the significant colocalization of LOXD1 and caveolin1, LOXD1 did not colocalize with clathrin heavy chains (Fig. 1D), suggesting that the trafficking

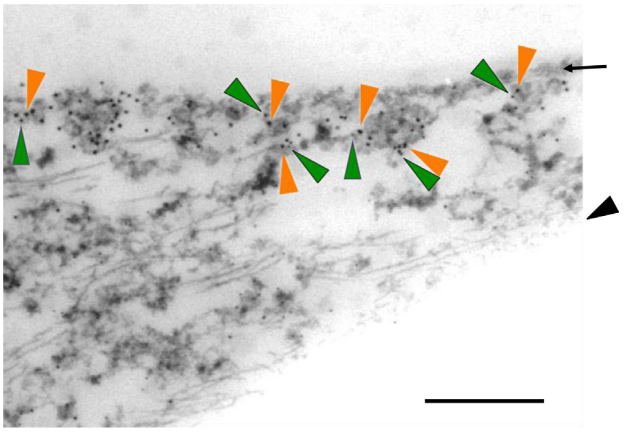

Fig. 2. Immuno-electron microscopy for LOXD1 and caveolin-1. Immunogold labeling for caveoin-1 (10 nm particle, orange arrowheads) and GFP (5 nm particle, green arrowheads) was performed in permeabilized cells. *Note*: The anti-GFP antibody recognizes the CFP and citrine of D1, components of LOXD1. A black arrow and an arrowhead indicate the apical site of the plasma membrane and a basal substratum attachment site, respectively. Bar = 500 nm. Images at lower magnifications and of a negative control are shown in Supplemental Fig. S4.

of LOXD1 was mediated mainly by caveolae, but not clathrin-coated pits. None of our other subcellular markers, including those specific for mitochondria (Fig. 1E), the trans-Golgi apparatus (Fig. 1F), cytosol (Fig. 1G), and the ER (Fig. 1H) colocalized with LOXD1. Importantly, subcellular distribution of LOXD1 was spatially distinct from the ER marker calreticulin. This was in contrast to the almost complete colocalization of calreticulin with the intra-ER Ca^{2+} sensor D1ER (Fig. 1I) [15], indicating LOXD1 detectable signals are different from intra-ER Ca^{2+} changes.

To further confirm that LOXD1 is targeted to caveolae, we performed immuno-electron microscopy, showing that a significant portion of LOXD1, as well as endogenous LOX-1 (Supplemental Fig. S3), was colocalized with caveolin-1 at morphologically apparent caveolar vesicles (Fig. 2). Thus, LOXD1 enabled us to specifically measure Ca^{2+} changes only inside closed caveolar vesicles.

Using the caveolar Ca^{2+} sensor LOXD1, we initially recorded the effect of ATP on Ca^{2+} levels inside closed caveolae by confocal FRET-imaging in a single endothelial cell expressing LOXD1. As anticipated, LOXD1 detected transient dose-dependent ATP-induced Ca^{2+} decreases in the presence of 1.2 mM extracellular calcium (Fig. 3A). Pseudo-colored ratio imaging at the subcellular level revealed that LOXD1 at some discrete cell edges detected ATP-induced transient decreases, most likely inside caveolae (Fig. 3B). These ATP-induced transient Ca^{2+} decreases were also seen even in the absence of extracellular calcium (Fig. 3C).

Next, we measured caveolar Ca^{2+} and cytosolic Ca^{2+} almost simultaneously in a cell doubly expressing the caveolar Ca^{2+} sensor, LOXD1, and the cytosolic red fluorescent Ca^{2+} sensing protein, RGECO. The graph shows that an ATP-induced, initial transient Ca^{2+} decrease was repeatedly observed inside caveolae (Fig. 4A). As a control experiment, we used the ER-targeted version of cameleon,

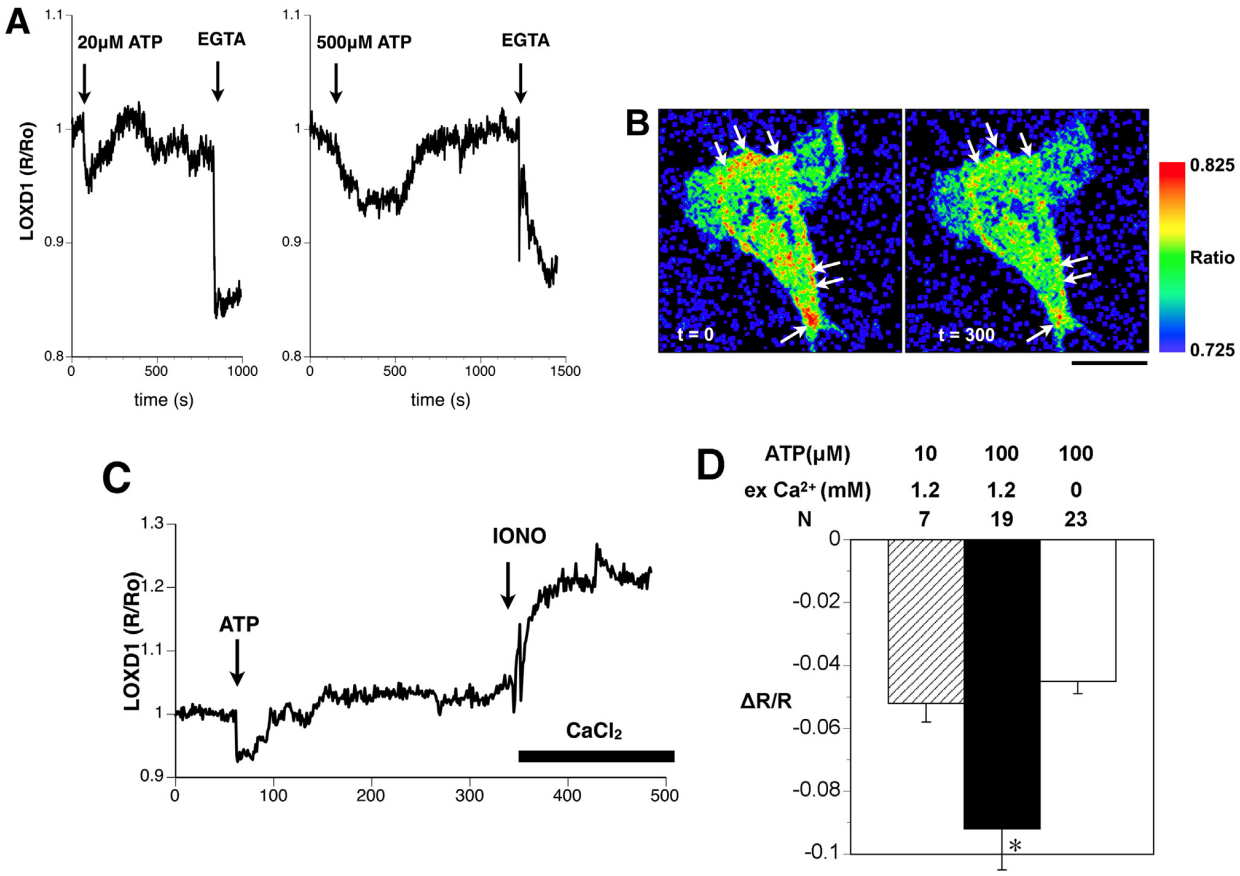

Fig. 3. LOXD1 detects an ATP-induced Ca^{2+} decrease. (A) An endothelial cell transiently expressing LOXD1 was stimulated with 20 μM or 500 μM ATP as indicated. (B) Pseudo-colored ratio images of basal (t = 0), 4 min after 500 μM ATP stimulation (t = 300). LOXD1 detected ATP-induced transient Ca^{2+} decreases at discrete cell edges (arrows). Bar = 10 μm. (C) An endothelial cell transiently expressing LOXD1 was stimulated with 100 μM ATP in the absence of extracellular Ca^{2+} for 5 min followed by re-addition of extracellular Ca^{2+} and 1 μM ionomycin (IONO) as indicated. (D) Quantification of ATP-induced decreases in FRET normalized to basal ratio (ΔR/R) in the presence (shaded and closed bars) or absence (open bar) of extracellular Ca^{2+} ($exCa^{2+}$). *p < 0.05, compared to 10 μM ATP stimulation, error bars = SE.

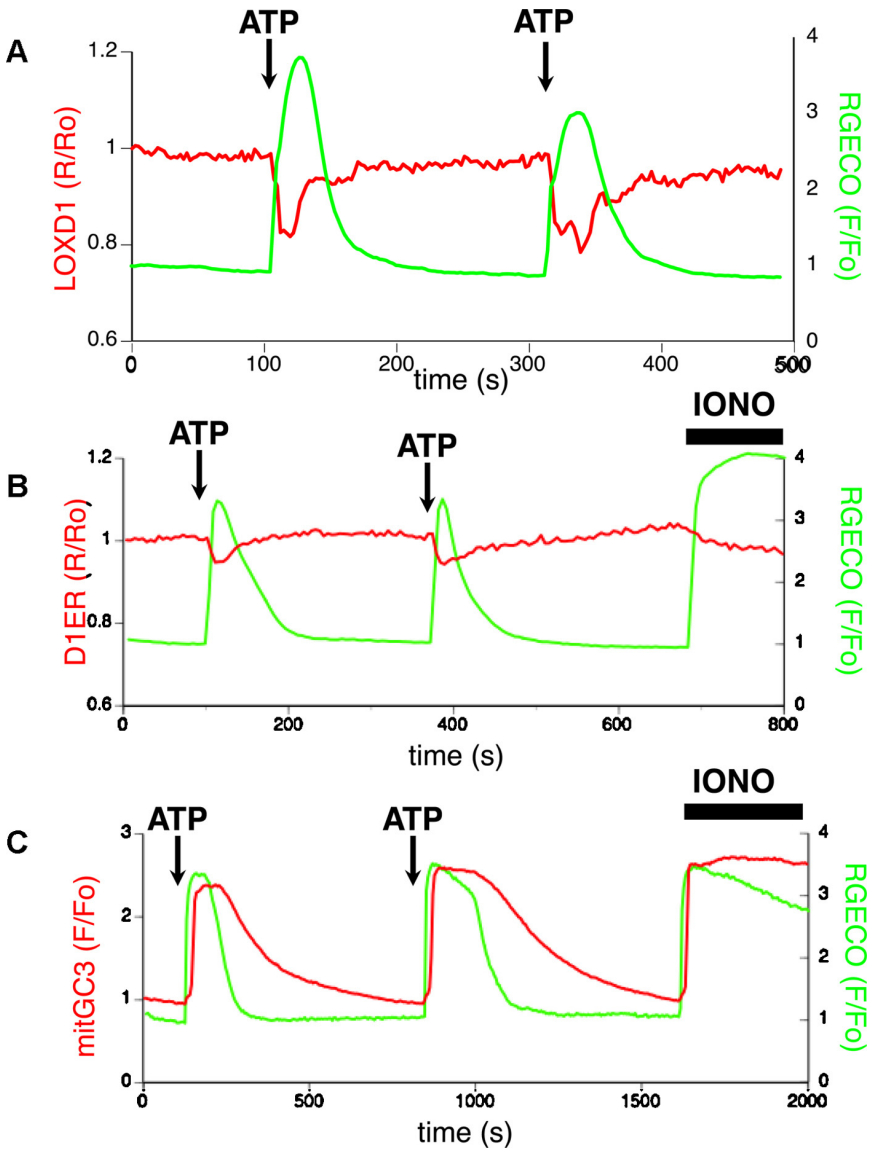

Fig. 4. Alternate recording of ATP-induced Ca^{2+} changes in caveolar vesicles and other intracellular subcompartments in the presence of extracellular Ca^{2+}. Alternate recording of Ca^{2+} in bulk cytosol and intracellular subcompartments including caveolae (A), the ER (B), and mitochondria (C), at intervals of 2.44 s using the Ca^{2+} sensing probes RGECO, LOXD1, D1ER, and mitGC3. RGECO-detected cytosolic Ca^{2+} changes are shown in green, and other intracellular subcompartments are shown in red. Single cells expressing two different Ca^{2+} sensors were repeatedly stimulated by 100 μM ATP in the presence of extracellular Ca^{2+}.

D1ER, and measured ER Ca^{2+} changes and cytosolic Ca^{2+} changes almost simultaneously (Fig. 4B). As anticipated, ATP transiently decreased Ca^{2+} in ER stores in parallel with cytosolic Ca^{2+} elevation. Interestingly, this observation of repeated ATP-induced transient ER Ca^{2+} decreases was highly comparable to intra-caveolar Ca^{2+} changes detected by LOXD1. In contrast to the ATP-induced Ca^{2+} decreases in caveolae vesicles or the ER, other subcompartments such as mitochondria showed transient Ca^{2+} increases, and did not work as Ca^{2+}-releasable Ca^{2+} store subcompartments (Fig. 4C).

To confirm that the ATP-induced FRET change was associated with caveolar structure, we silenced caveolin-1 expression by transient expression of caveolin-1-specific shRNA in an RFP vector. Decreased expression of caveolin-1 was confirmed by caveolin-1 immunostaining in RFP expressing cells (Supplemental Fig. S5). ATP-induced transient FRET decreases were abolished in cells simultaneously expressing LOXD1 and caveolin-1-specific shRNA (Fig. 5), suggesting the Ca^{2+} responses were possibly associated with caveolar structure.

Finally, we performed X-ray microanalysis of calcium precipitation using the pyroantimonate method to confirm that caveolar vesicles contain high amounts of calcium. It is known that the precipitate contains a large amount of calcium if the peak X-ray energy used is around 3620 eV. As shown in the micrographs, spot analysis of caveolae-rich plasma membranes revealed a typical peak pattern for calcium (Fig. 6A and B). The density of pyroantimonate precipitation inside caveolae decreased in response to ATP (Fig. 6C, Supplemental Fig. S6), suggesting that caveolae are Ca^{2+}-releasable Ca^{2+} store subcompartments (Fig. 7). Confirmatively, in situ proximal ligation assays and co-immunoprecipitation analysis revealed that caveolin-1 was colocalized both with the PMCA Ca^{2+} pump and IP_3 receptor type 1 (Supplemental Figs. S7 and S8).

4. Discussion

We targeted a FRET-based Ca^{2+} sensor to inside caveolae and demonstrated in intact endothelial cells that subplasmalemmal

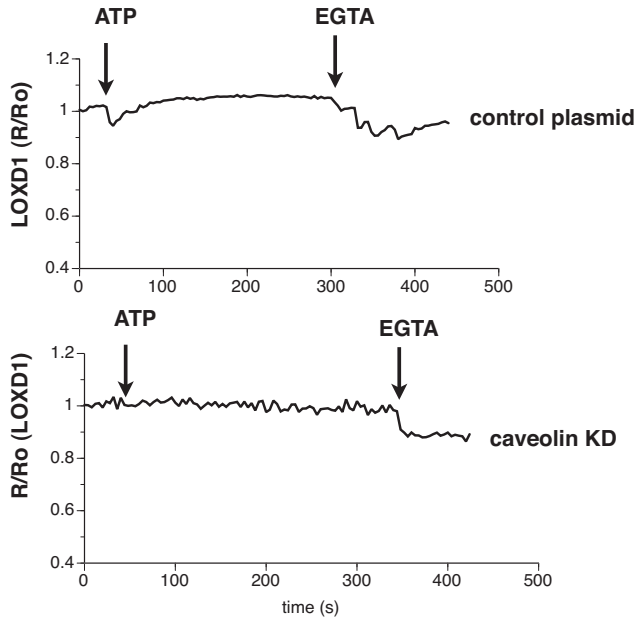

Fig. 5. Knockdown of endogenous caveolin-1 abolishes ATP-induced Ca^{2+} changes. FRET time lapse was recorded in endothelial cells simultaneously expressing LOXD1 and caveolin-1-specific shRNA or negative control scramble shRNA in RFP vector.

caveolar vesicles work as Ca^{2+}-releasable Ca^{2+} store subcompartments. The key issue to be resolved in this study involved developing a method for targeting a Ca^{2+} sensor to the intracaveolar space. To achieve this aim, we utilized the endocytic pathway of LOX-1, which is a single membrane spanning receptor for oxidized low-density lipoprotein (LDL) with its C-terminus on the outside of the plasma membrane or inside trafficking vesicles [17]. Previous reports suggest that LOX-1 is internalized by a clathrin-independent and dynamin-dependent pathway [18] and that dynamin mediates caveolae internalization [19]. More recent reports from different groups demonstrated that LOX-1 is biochemically present in caveolae-enriched lipid rafts and that caveolae mediate endocytosis of oxidized LDL in endothelial cells [20] [21]. We also confirmed by electron microscopy studies that endogenous LOX-1 is clearly colocalized with caveolin-1 at morphologically apparent caveolar membranes (Supplemental Fig. S3). Thus, endocytosis and trafficking of LOX-1 may be closely associated with caveolae, and we predicted that the Ca^{2+} sensor D1 would be targeted to endocytosed, closed caveolar vesicles by expressing its fusion protein LOXD1. As expected, a large portion of D1 was outside the plasma membrane and some portion was present as single or racemous vesicles (Supplemental Fig. S2) that were clearly colocalized with the caveolar marker caveolin-1, but not clathrin heavy chains. These results suggested that the trafficking of LOXD1 was mediated mainly by caveolae, but not clathrin coated pits. Colocalization of LOXD1 with caveolin-1 was confirmed by immunofluorescence and immune electron microscopy. Because the FRET status of D1 expressed outside the plasma membrane remained unchanged by the constant Ca^{2+} levels in the recording medium, FRET changes in LOXD1-expressing cells led us to specifically measure Ca^{2+} dynamics inside caveolar vesicles. The Ca^{2+} sensor D1 was originally made to detect intra ER Ca^{2+} changes ranging from about 10 μM to several hundred μM [15], and was found in the present study to be suitable for Ca^{2+} measurements inside caveolae.

Because D1ER is almost completely expressed in the ER (Fig. 1H), we can assume the intra-ER Ca^{2+} level to be 128 μM (Supplemental Table). In contrast, the conversion of FRET levels in caveolae to $[Ca^{2+}]$ is difficult owing to background FRET at the non-caveolar locations of some D1. Taking this into account, we tried to calibrate the LOXD1-detectable average $[Ca^{2+}]$ in a single cell in the presence or absence of extracellular Ca^{2+} (Supplemental Fig. S9 and Table). We assumed that intracaveolar Ca^{2+} levels are between these ranges (21–153 μM) and that $[Ca^{2+}]$ inside some populations of caveolae may be comparable to intra-ER Ca^{2+} levels. However, caveolar Ca^{2+} storage capacity is probably much lower than the ER in view of the enclosed volumes.

Earlier studies using the pyroantimonate method demonstrated that the density of calcium precipitation in subplasmalemmal caveolae was clearly in concert with the excitation–contraction cycle, suggesting release and re-loading of Ca^{2+} across the caveolar membrane in excitable cells [22,23]. In the present study, we confirmed using the same technique that caveolar vesicles contain high amounts of calcium and that the precipitate density decreased in response to ATP in non-excitable endothelial cells. Furthermore, FRET-imaging using LOXD1 successfully detected intra-caveolar Ca^{2+} changes in response to ATP at some discrete cell edges, indicating that caveolae are Ca^{2+} releasable Ca^{2+} store subcompartments. Interestingly, the recorded Ca^{2+} dynamics inside caveolae were very similar to those in the ER, a major spatially distinct Ca^{2+} store compartment. In contrast, Ca^{2+} dynamics in another subcellular compartment, mitochondria, were similar to bulk cytosolic Ca^{2+} and did not work as Ca^{2+}-releasable Ca^{2+} stores. Molecular components essential for the ER to work as a Ca^{2+}-releasable Ca^{2+} store compartment are the IP_3 receptor and the Ca^{2+} pump on the ER membrane [24], playing their roles for extrusion and sequestration of Ca^{2+}, respectively. Previous reports clearly demonstrate by immunoelectron microscopy that an IP_3 receptor-like protein [10] and a Ca^{2+}-ATPase [11] are abundantly localized at caveolae in endothelial cells. More recently, caveolin-1 was shown to be co-immunoprecipitated with the IP_3 receptor type 1 in smooth muscle cells [25]. We also confirmed by in situ proximal ligation assay and co-immunoprecipitation analysis that plasma membrane Ca^{2+}-ATPase and IP_3 receptor type 1 are colocalized with caveolin-1 (Supplemental Figs. S7 and S8). Thus, our observation in the present study is consistent with the proposal by Dr. Fujimoto that caveolae work as Ca^{2+}-releasable Ca^{2+} store subcompartments spatially distinct from the ER. Previously, in other cell types, different Ca^{2+} probes have been used to measure Ca^{2+} levels in subcellular compartments including the ER, mitochondria, Golgi, endosome, and secretary granules (see review [26]). The Golgi apparatus [27], isolated pancreatic zymogen granules [28], isolated mucin granules [29], isolated mast cell granules [30], and acrosomes of sperm [31] were responsive to IP_3 for releasing Ca^{2+}, while granules in neuroendocrine cells [32] and insulin-containing vesicles in pancreatic beta cells [32] were not. Because caveolae are preferential sites for PI hydrolysis via Gq-coupled phospholipase C (PLC) activation [33] and caveolin-rich cell edges are initiation sites in IP_3-dependent Ca^{2+} releases from the ER [5], ATP-induced transient Ca^{2+} decreases inside caveolae are probably mediated by IP_3. Plasma membrane Ca^{2+}-ATPase is a high affinity, low capacity Ca^{2+} pump, and represents a primary pathway for Ca^{2+} extrusion out of the cell following intracellular Ca^{2+} elevation [34]. Interestingly, plasma membrane Ca^{2+}-ATPase is internalized through a lipid raft endocytic pathway during Xenopus oocyte maturation and the rate of Ca^{2+} extrusion is slowed down [35,36], supporting our and Dr. Fujimoto's proposal that subplasmalemmal caveolar Ca^{2+} storage is maintained by Ca^{2+}-ATPase activity.

Ca^{2+} delivery from subplasmalemmal caveolae can modify spatiotemporal Ca^{2+} signaling and affect endothelial function. Because caveolae are mobile and their distribution is highly polarized, especially in migrating endothelial cells [37], Ca^{2+} release from caveolar vesicles may contribute to the Ca^{2+} wave initiation at caveolin-rich cell edges by priming the sensitization of local IP_3 receptors on

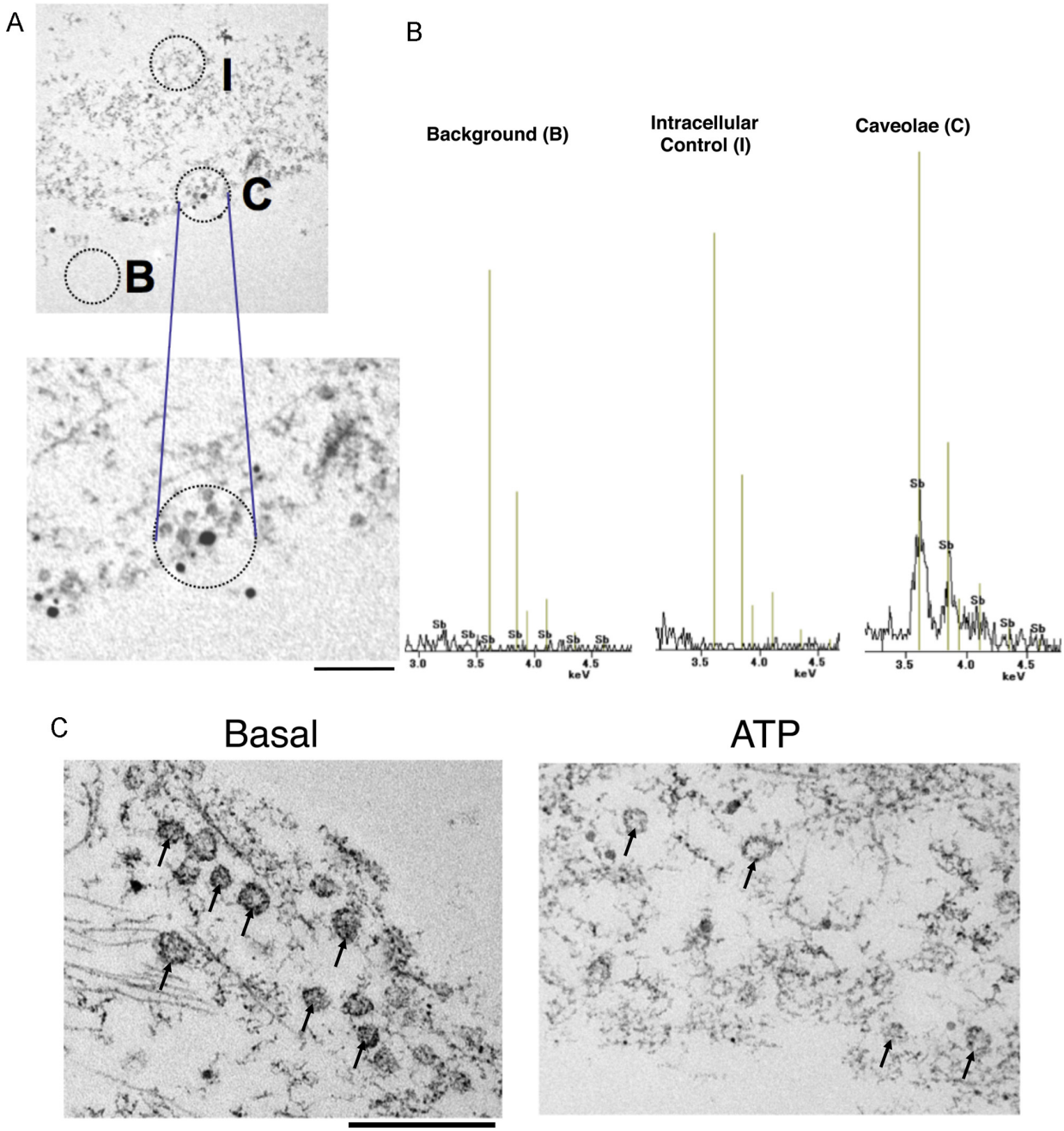

Fig. 6. X-ray microanalysis of calcium precipitation by pyroantimonate methods. Spot microanalysis of the caveolae-rich plasma membranes (C), intracellular control regions (I), and non-cellular background (B) was performed. Bar = 500 μm. (B) Energy spectrum of X-ray microanalysis. Caveolae-rich plasma membranes revealed a typical peak pattern for calcium. Note that the precipitate contains a high amount of calcium if the peak X-ray energy used is around 3620 eV. (C) Micrographs before (Basal) and after 100 μM ATP stimulation (ATP) in the absence of extracellular Ca^{2+}. Note the density of pyroantimonate precipitation inside caveolae decreased in response to ATP (arrows). Bar = 500 μm. Images of these regions at lower magnification are shown in Supplemental Fig. S6.

the ER [7]. Consistent with this hypothesis, a recent report demonstrated that caveolin-1 deficiency, which should induce complete disappearance of morphological caveolae, impairs Ca^{2+} release but not IP_3 production in endothelial cells [38]. Furthermore, because caveolar vesicles are known to travel on microtubules to different regions of the cell [39], quantal delivery of caveolar Ca^{2+} may locally affect Ca^{2+} dependent effectors such as eNOS, which is closely regulated by Ca^{2+} and caveolin-1 at endothelial caveolae [40]. In fact, spatial confinement of different nitric oxide (NO) synthase isoforms and NO signaling could allow independent effects on the phenotype of cardiac cells [41]. Finally, Ca^{2+} release from ER Ca^{2+} stores are known to stress cells, known as ER-stress, by misfolding of synthesized proteins. Thus, Ca^{2+} mobilization from non-ER Ca^{2+} store subcompartments may be harmless to cells during Ca^{2+}-dependent local signal activation around caveolae.

Ca^{2+} binding proteins such as calreticulin or calsequestrin are essential for Ca^{2+} storage in membrane-closed compartments. Although immune-reactivity for calreticulin at the cytoplasmic site

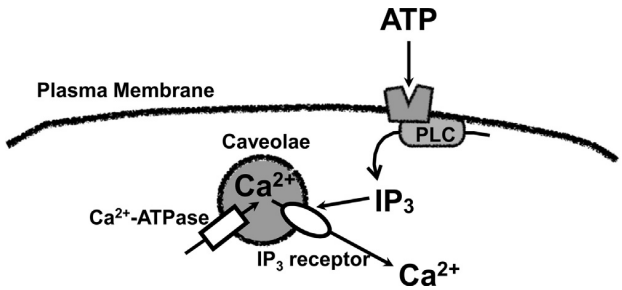

Fig. 7. Proposed model of caveolae as Ca^{2+}-releasable Ca^{2+} store subcompartments.

of caveolae was detected [42], Ca^{2+} binding proteins inside caveolae remain unidentified and the capacity of Ca^{2+} storage inside caveolae is not known. Furthermore, it remains unclear how dynamic caveolar budding and pinching off from the plasma membrane affects store-operated Ca^{2+} entry. Further investigations are necessary to clarify such issues.

5. Conclusion

In this study, we directly measured intra-caveolar Ca^{2+} dynamics by targeting the FRET-based Ca^{2+} sensor and by pyroantimonate precipitation methods. We found that subplasmalemmal caveolae function as Ca^{2+}-releasable Ca^{2+} stores in response to ATP. This intracellular local Ca^{2+} delivery system may contribute to the highly complex spatiotemporal organization of Ca^{2+} signaling, and may increase the versatility of endothelial functions with less Ca^{2+} depletion in ER-Ca^{2+} stores.

Disclosure

None.

Acknowledgments

We thank Ms. Seiko Kawai and Ms. Miho Miyazawa for their technical assistance. This work was supported by grants from the Ministry of Education, Culture, Sports, Science and Technology of Japan, Grant-in Aid for Scientific Research (21590948, 2009–2011) and Novartis Pharmaceuticals. We are grateful to Drs. T. Sawamura (National Cardiovascular Center Research Institute, Osaka, Japan), T. Tsien (Howard Hughes Medical Institute, UCSD, La Jolla, CA, USA), L. Looger (Howard Hughes Medical Institute, Ashburn, VA, USA), and R.E. Campbell (University of Alberta, Edmonton, Alberta, Canada) for providing cDNA for bovine LOX-1 and expression vectors for yellow cameleon mutants, GCaMP3, and RGECO, respectively.

Appendix A. Supplementary data

Supplementary data associated with this article can be found, in the online version, at http://dx.doi.org/10.1016/j.ceca.2013.09.002.

References

[1] T. Michel, P.M. Vanhoutte, Cellular signaling and NO production, Pflugers Archiv: European Journal of Physiology 459 (2010) 807–816.
[2] M.J. Berridge, M.D. Bootman, H.L. Roderick, Calcium signalling: dynamics, homeostasis and remodelling, Nature Reviews Molecular Cell Biology 4 (2003) 517–529.
[3] G. Rath, C. Dessy, O. Feron, Caveolae, caveolin and control of vascular tone: nitric oxide (NO) and endothelium derived hyperpolarizing factor (EDHF) regulation, Journal of Physiology and Pharmacology: An Official Journal of the Polish Physiological Society 60 (Suppl. 4) (2009) 105–109.
[4] R.G. Anderson, The caveolae membrane system, Annual Review of Biochemistry 67 (1998) 199–225.
[5] M. Isshiki, J. Ando, R. Korenaga, H. Kogo, T. Fujimoto, T. Fujita, A. Kamiya, Endothelial Ca^{2+} waves preferentially originate at specific loci in caveolin-rich cell edges, Proceedings of the National Academy of Sciences of the United States of America 95 (1998) 5009–5014.
[6] M. Isshiki, Y.S. Ying, T. Fujita, R.G. Anderson, A molecular sensor detects signal transduction from caveolae in living cells, Journal of Biological Chemistry 277 (2002) 43389–43398.
[7] M. Isshiki, R.G. Anderson, Calcium signal transduction from caveolae, Cell Calcium 26 (1999) 201–208.
[8] M. Isshiki, R.G. Anderson, Function of caveolae in Ca^{2+} entry and Ca^{2+}-dependent signal transduction, Traffic 4 (2003) 717–723.
[9] B. Pani, B.B. Singh, Lipid rafts/caveolae as microdomains of calcium signaling, Cell Calcium 45 (2009) 625–633.
[10] T. Fujimoto, S. Nakade, A. Miyawaki, K. Mikoshiba, K. Ogawa, Localization of inositol 1,4,5-trisphosphate receptor-like protein in plasmalemmal caveolae, Journal of Cell Biology 119 (1992) 1507–1513.
[11] T. Fujimoto, Calcium pump of the plasma membrane is localized in caveolae, Journal of Cell Biology 120 (1993) 1147–1157.
[12] P.W. Shaul, E.J. Smart, L.J. Robinson, Z. German, I.S. Yuhanna, Y. Ying, R.G. Anderson, T. Michel, Acylation targets emdothelial nitric-oxide synthase to plasmalemmal caveolae, Journal of Biological Chemistry 271 (1996) 6518–6522.
[13] L. Tian, S.A. Hires, T. Mao, D. Huber, M.E. Chiappe, S.H. Chalasani, L. Petreanu, J. Akerboom, S.A. McKinney, E.R. Schreiter, C.I. Bargmann, V. Jayaraman, K. Svoboda, L.L. Looger, Imaging neural activity in worms, flies and mice with improved GCaMP calcium indicators, Nature Methods 6 (2009) 875–881.
[14] Y. Zhao, S. Araki, J. Wu, T. Teramoto, Y.F. Chang, M. Nakano, A.S. Abdelfattah, M. Fujiwara, T. Ishihara, T. Nagai, R.E. Campbell, An expanded palette of genetically encoded Ca^{2+} indicators, Science 333 (2011) 1888–1891.
[15] A.E. Palmer, C. Jin, J.C. Reed, R.Y. Tsien, Bcl-2-mediated alterations in endoplasmic reticulum Ca^{2+} analyzed with an improved genetically encoded fluorescent sensor, Proceedings of the National Academy of Sciences of the United States of America 101 (2004) 17404–17409.
[16] M. Isshiki, A. Mutoh, T. Fujita, Subcortical Ca^{2+} waves sneaking under the plasma membrane in endothelial cells, Circulation Research 95 (2004) e11–e21.
[17] T. Sawamura, N. Kume, T. Aoyama, H. Moriwaki, H. Hoshikawa, Y. Aiba, T. Tanaka, S. Miwa, Y. Katsura, T. Kita, T. Masaki, An endothelial receptor for oxidized low-density lipoprotein, Nature 386 (1997) 73–77.
[18] J.E. Murphy, R.S. Vohra, S. Dunn, Z.G. Holloway, A.P. Monaco, S. Homer-Vanniasinkam, J.H. Walker, S. Ponnambalam, Oxidised LDL internalisation by the LOX-1 scavenger receptor is dependent on a novel cytoplasmic motif and is regulated by dynamin-2, Journal of Cell Science 121 (2008) 2136–2147.
[19] P. Oh, D.P. McIntosh, J.E. Schnitzer, Dynamin at the neck of caveolae mediates their budding to form transport vesicles by GTP-driven fission from the plasma membrane of endothelium, Journal of Cell Biology 141 (1998) 101–114.
[20] S.W. Sun, X.Y. Zu, Q.H. Tuo, L.X. Chen, X.Y. Lei, K. Li, C.K. Tang, D.F. Liao, Caveolae and caveolin-1 mediate endocytosis and transcytosis of oxidized low density lipoprotein in endothelial cells, Acta Pharmacologica Sinica 31 (2010) 1336–1342.
[21] M. Kumano-Kuramochi, Q. Xie, S. Kajiwara, S. Komba, T. Minowa, S. Machida, Lectin-like oxidized LDL receptor-1 is palmitoylated and internalizes ligands via caveolae/raft-dependent endocytosis, Biochemical and Biophysical Research Communications 434 (2013) 594–599.
[22] L.M. Popescu, I. Diculescu, U. Zelck, N. Ionescu, Ultrastructural distribution of calcium in smooth muscle cells of guinea-pig taenia coli. A correlated electron microscopic and quantitative study, Cell and Tissue Research 154 (1974) 357–378.
[23] H. Sugi, S. Suzuki, T. Daimon, Intracellular calcium translocation during contraction in vertebrate and invertebrate smooth muscles as studied by the pyroantimonate method, Canadian Journal of Physiology and Pharmacology 60 (1982) 576–587.
[24] M.J. Berridge, P. Lipp, M.D. Bootman, The versatility and universality of calcium signalling, Nature Reviews Molecular Cell Biology 1 (2000) 11–21.
[25] A. Adebiyi, D. Narayanan, J.H. Jaggar, Caveolin-1 assembles type 1 inositol 1,4,5-trisphosphate receptors and canonical transient receptor potential 3 channels into a functional signaling complex in arterial smooth muscle cells, Journal of Biological Chemistry 286 (2011) 4341–4348.
[26] O. Gerasimenko, A. Tepikin, How to measure Ca^{2+} in cellular organelles? Cell Calcium 38 (2005) 201–211.
[27] P. Pinton, T. Pozzan, R. Rizzuto, The Golgi apparatus is an inositol 1,4,5-trisphosphate-sensitive Ca^{2+} store, with functional properties distinct from those of the endoplasmic reticulum, EMBO Journal 17 (1998) 5298–5308.
[28] O.V. Gerasimenko, J.V. Gerasimenko, P.V. Belan, O.H. Petersen, Inositol trisphosphate and cyclic ADP-ribose-mediated release of Ca^{2+} from single isolated pancreatic zymogen granules, Cell 84 (1996) 473–480.
[29] T. Nguyen, W.C. Chin, P. Verdugo, Role of Ca^{2+}/K^{+} ion exchange in intracellular storage and release of Ca^{2+}, Nature 395 (1998) 908–912.
[30] I. Quesada, W.C. Chin, J. Steed, P. Campos-Bedolla, P. Verdugo, Mouse mast cell secretory granules can function as intracellular ionic oscillators, Biophysical Journal 80 (2001) 2133–2139.
[31] G. De Blas, M. Michaut, C.L. Trevino, C.N. Tomes, R. Yunes, A. Darszon, L.S. Mayorga, The intraacrosomal calcium pool plays a direct role in acrosomal exocytosis, Journal of Biological Chemistry 277 (2002) 49326–49331.

[32] K.J. Mitchell, F.A. Lai, G.A. Rutter, Ryanodine receptor type I and nicotinic acid adenine dinucleotide phosphate receptors mediate Ca^{2+} release from insulin-containing vesicles in living pancreatic beta-cells (MIN6), Journal of Biological Chemistry 278 (2003) 11057–11064.
[33] L.J. Pike, L. Casey, Localization and turnover of phosphatidylinositol 4,5-bisphosphate in caveolin-enriched membrane domains, Journal of Biological Chemistry 271 (1996) 26453–26456.
[34] D. Guerini, L. Coletto, E. Carafoli, Exporting calcium from cells, Cell Calcium 38 (2005) 281–289.
[35] W. El-Jouni, B. Jang, S. Haun, K. Machaca, Calcium signaling differentiation during Xenopus oocyte maturation, Developmental Biology 288 (2005) 514–525.
[36] A.F. El-Yazbi, W.J. Cho, R. Schulz, E.E. Daniel, Calcium extrusion by plasma membrane calcium pump is impaired in caveolin-1 knockout mouse small intestine, European Journal of Pharmacology 591 (2008) 80–87.
[37] M. Isshiki, J. Ando, K. Yamamoto, T. Fujita, Y. Ying, R.G. Anderson, Sites of Ca^{2+} wave initiation move with caveolae to the trailing edge of migrating cells, Journal of Cell Science 115 (2002) 475–484.
[38] T. Murata, M.I. Lin, R.V. Stan, P.M. Bauer, J. Yu, W.C. Sessa, Genetic evidence supporting caveolae microdomain regulation of calcium entry in endothelial cells, Journal of Biological Chemistry 282 (2007) 16631–16643.
[39] K.A. McMahon, H. Zajicek, W.P. Li, M.J. Peyton, J.D. Minna, V.J. Hernandez, K. Luby-Phelps, R.G. Anderson, SRBC/cavin-3 is a caveolin adapter protein that regulates caveolae function, EMBO Journal 28 (2009) 1001–1015.
[40] J.B. Michel, O. Feron, D. Sacks, T. Michel, Reciprocal regulation of endothelial nitric-oxide synthase by Ca^{2+}-calmodulin and caveolin, Journal of Biological Chemistry 272 (1997) 15583–15586.
[41] L.A. Barouch, R.W. Harrison, M.W. Skaf, G.O. Rosas, T.P. Cappola, Z.A. Kobeissi, I.A. Hobai, C.A. Lemmon, A.L. Burnett, B. O'Rourke, E.R. Rodriguez, P.L. Huang, J.A. Lima, D.E. Berkowitz, J.M. Hare, Nitric oxide regulates the heart by spatial confinement of nitric oxide synthase isoforms, Nature 416 (2002) 337–339.
[42] R. Nomura, T. Aoki, H. Hagiwara, T. Senda, T. Fujimoto, Anti-calreticulin antibody binds to a membrane protein in caveolae, Acta Histochemica et Cytochemica 38 (2005) 43–52.